

Numerical Simulation of Explosion on Barre Granite

Kshitiz Joshi ^a, Santosh Kumar Yadav ^b

^{a, b} Department of Civil Engineering, Pulchowk Campus, IOE, Tribhuvan University, Nepal

✉ ^a kshitiz.joshi1@gmail.com, ^b santosh.yadav@pcampus.edu.np

Abstract

Existing studies have used the methods of the theoretical analysis, field test, numerical simulation and model test to study the rock blasting damage and blast-induced vibration. Among them, numerical simulation has been used by many researchers. The study of rock blasting finds its use especially in the civil engineering projects involving drill and blast tunneling. Proper understanding of blasting process including blast wave propagation and cracks formation during explosion is important to optimize the blast design process.

Finite Element Method (FEM) has been used for numerical simulation of the rock blasting process. The data from a laboratory based experiment is used for simulating blast in the numerical model. Proper selection of constitutive models for the rocks is important to simulate the brittle nature of the rocks and to accurately model their interaction with explosives. Two different models, Johnson-Holmquist 2 (JH-2) damage model and RHT damage model for rocks, combined with Arbitrary Lagrangian Eulerian Model (ALE) Model for rock were used. The performances of both the model were compared with the laboratory experiments. The crack patterns generated by both the model were found in conformity with the results of the lab scale experiments performed with Barre Granite. It was found that the RHT model can more accurately model the rock blasting process compared with the JH-2 model.

Keywords

Rock blasting, RHT model, JH-2 model, Damage pattern

1. Introduction

Rock blasting is extensively used in civil engineering projects. In the hilly terrain of Nepal, it has been used for a long time in road construction. Similarly, Drill and blast is very common method of tunneling in Nepal. Apart from a few projects constructed with the Tunnel Boring Machines (TBMs), majority of the tunnels have been constructed with drill and blast methodology.

In the drill and blast method of tunneling, the tunnel advance is made through drilling several holes in the rock, loading them with explosives, detonating the explosives and subsequent removal of rocks and muck. The variables involved in this method include type of rock, type of explosives, method of cutting such as parallel cut, wedge cut, powder factor, detonation time and delays, burden, hole diameter and decoupling ratio. Precise and detailed calculations are required to optimize the blast efficiency to obtain required cross section through blasting.

In this context, very few research have been made to understand and study the blasting phenomenon in rocks in Nepal. The experimental analysis is extremely complicated due to difficulty in obtaining information from the blasting due to transient nature of the blast as well as safety issues during blasting. However, it is imperative to understand the blasting process and the manner of crack propagation and destruction process of rocks subject to the blast loading. Numerical analysis is a very effective method to understand and simulate the rock blasting phenomena.

To better understand the explosion process, it is necessary to accurately simulate the rock explosion. Several attempts have been made to numerically model the blasting process. The

Reidel-Heirmaier-Thoma (RHT) model was employed for multi-hole blasting, and afterward, the simulation outcomes were matched against experimental observations [1]. Smooth Particle Hydrodynamics (SPH) and Finite Element Method (FEM) method was used along with the RHT model of rock to investigate the damage zone and fracture characteristics of rock by [2]. The crack propagation was studied using the CSCM model for the rocks [3]. The RHT model and HJC model were compared in blast simulation of granite and RHT model was suggested for the simulation of cyclic blasting problems by [4]. The integration of Discrete Element Method (DEM) and Smoothed-Particle Hydrodynamics (SPH) was utilized for the purpose of simulating rock blasting [5]. The utilization of the Finite Element method was employed to examine the impact of time delays in blasting on the formation of cracks [6].

It is important to understand the Constitutive models used for blasting process, especially for rocks and explosives. For rocks, the constitutive model must be able to accurately depict the brittle nature of the rocks. Furthermore, the Fluid Structure interaction in the form of interaction of blasting waves with the rocks and subsequent damage must be accurately modelled. Various methods of modeling the rocks and explosives in the form of Lagrangian, Eulerian and Arbitrary Lagrangian Eulerian (ALE) as well as Smooth Particle Hydrodynamics (SPH) method have been used. There is common consensus for modeling explosives using Material High explosive burn. However, for rocks several constitutive models, namely, Johnson-Holmquist (JH-2) model, Reidel-Heirmaier-Thoma (RHT) model, JHC model, Taylor-Chen-Kuzmaul (TCK) model, Continuous Surface Cap Model (CSCM) model have been in use. Very few studies have been made to compare the constitutive models

and their ability to simulate the rock explosion. In this paper, an effort has been undertaken to evaluate the effectiveness of two constitutive models, namely, the JH-2 damage model and the RHT damage model, in their capacity to replicate explosive damage when compared to experimental findings conducted in a laboratory setting. The two models are compared and results are presented.

2. Numerical Model

A laboratory scale test was performed by [7] using a cylindrical rock sample of Barre granite with a diameter of 14.4 cm and a height of 15 cm. A borehole was created at the sample's central point, and within it, an explosive device enclosed within a copper tube having an external diameter of 6.45 mm was inserted. The borehole contained air, a polyethylene sheath, and Pentaerythritol tetranitrate (PETN, an explosive material) along with Copper. Figure 1 shows the sample from the [7] experiment while Figure 2 shows the plan view of the different materials used in the experiment and their respective diameters.

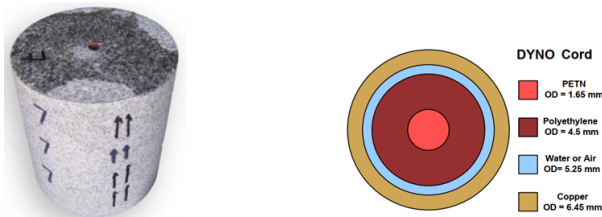


Figure 1: Overall view of the sample from Banadaki(2010) experiment

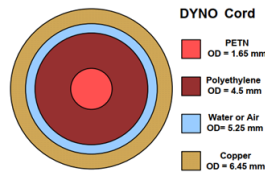
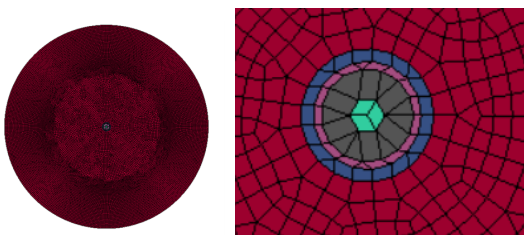


Figure 3: 3d view of the FEM model



(a) Overall plan view of all the elements (b) Exploded view of elements

Figure 4: Plan View of the FEM Model

Table 1: Parameters of PETN, Wang (2018)

SN	Parameter	Details
1	Density	1630
2	Velocity of Detonation	6690
3	Chapman Gouget Pressure	1.6e10
4	A(Pa)	5.86e11
5	B (Pa)	2.16e10
6	R1	5.81
7	R2	1.77
8	w	0.282
9	V	1
10	Eo (J/m3)	7.38e9

Table 2: Parameters of Polyethylene, Wang (2018)

SN	Parameter	Details
1	Density (kg/m3)	79
2	Bulk sound speed (m/s)	290.1
3	Material constant, S1	1.481
4	Material constant, S2	0
5	Material constant, S3	0

Table 3: Parameters of Copper, Wang (2018)

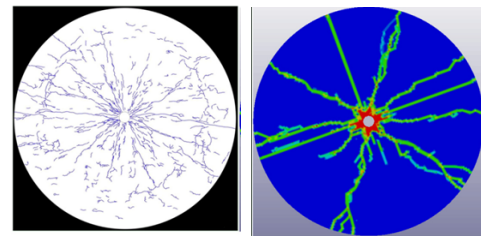
SN	Parameter	Details
1	Density (kg/m3)	8330
2	Young's Modulus (Pa)	1.38e10
3	Poisson's ratio	0.35
4	A(Pa)	8.963e7
5	B(Pa)	2.916e8
6	N	0.31
7	C	0.025
8	M	1.09
9	Melting Temperature	1200
10	Room Temperature	30
11	Specific Heat	4400
12	C (Gruneisen EOS)	0.394
13	S1	1.489
14	S2	0
15	S3	0
16	Gamma	2.02
12	A (Gruneisen EOS)	0.47
13	Eo	0

Table 4: Parameters of Air, Wang (2018)

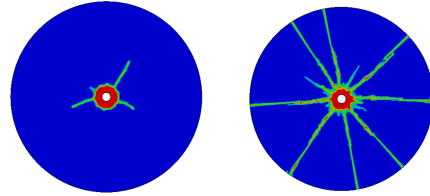
SN	Parameter	Details
1	Density (kg/m3)	1.29
2	PC	0
3	C0	0
4	C1	0
5	C2	0
6	C3	5.0
7	C4	0.4
8	C5	0.4
9	C6	0
10	Eo (Pa)	2.5e5
11	Vo	1

Table 5: Parameters of RHT model, Li (2023)

SN	Parameter	Details
1	Density	2660
2	Elastic shear modulus (Pa)	20.28
3	Eroding Plastic Strain	2.0
4	Parameter for polynomial EOS, Bo	1.22
5	Parameter for Polynomial EOS, B1	1.22
6	Parameter for Polynomial EOS, T1 (Pa)	51.57e9
7	Parameter for Polynomial EOS, T2 (Pa)	0.0
8	Failure Surface Parameter, A	2.57
9	Failure Surface Parameter, N	0.75
10	Compressive Strength, (Pa)	259e6
11	Crush Strength PEL (Pa)	172.67e6
12	Relative shear strength	0.21
13	Relative tensile strength	0.10
14	Load Angle dependence factor, Qo	0.68
15	Load Angle dependence factor, B	0.05
16	Reference compressive strain EOS (s-1)	3e-5
17	Reference tensile strain rate ETC (s-1)	3e-6
18	Break compressive strain rate EC (s-1)	3e25
19	Break tensile strain ET (s-1)	3e25
20	Compressive strain rate dependence exponent	0.026
21	Tensile strain rate dependence exponent	0.007
22	Volumetric plastic strain fraction in tension	0.001
23	Compressive yield surface parameter	0.53
24	Tensile yield surface parameter	0.70
25	Shear modulus reductio factor	0.50
26	Damage parameter, D1	0.04
27	Damage parameter, D2	1.00
28	Minimum damaged residual strain	0.015
29	Residual surface parameter	1.60
30	Residual surface parameter, NF	0.61
31	Gruneisen Gamma	0.0
32	Hugoniot Polynomial coefficient, A1 (Pa)	51.57e9
33	Hugoniot Polynomial Coefficient, A2 (Pa)	60.23e9
34	Hugoniot Polynomial Coefficient, A3 (Pa)	9.76e9
35	Compaction Pressure, PCO(Pa)	6e9
36	Porosity exponent NP	3.0
36	Initial Porosity	1.006

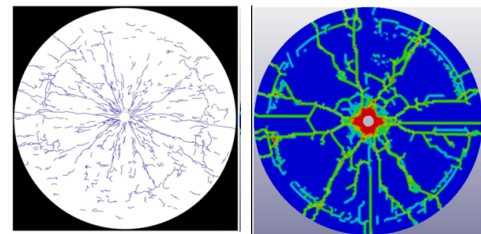


(a) Banadaki (2010) experiment (b) Wang (2018) model

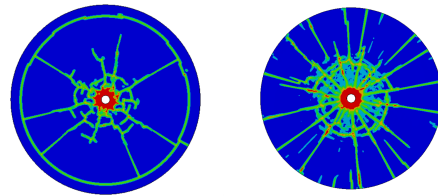


(c) JH2 model (d) RHT model

Figure 5: Damage pattern in the top of the sample



(a) Banadaki (2010) experiment (b) Wang (2018) model



(c) JH2 model (d) RHT model

Figure 6: Damage pattern in the bottom of the sample

Table 6: Parameters of JH-2 model, Wang (2018)

SN	Parameter	Details
1	Density	2660
2	Shear Modulus (G)	21.9e9
3	Intact Strength Coefficient, A	1.25
4	Fractured Strength Coefficient, B	0.68
5	Strain Rate Coefficient, C	0.005
6	Fractured Strength Coefficient, M	0.83
7	Intact Strength Exponent, N	0.68
8	Maximum Tensile Strength, T	57e6
9	Hugoniot Elastic Limit, (HEL) (Pa)	4.5e9
10	HEL Pressure, Pa	2.93e9
11	Bulk Factor	1
12	Damage Coefficient, D1	0.008
13	Damage Coefficient, D2	0.44
14	Bulk modulus, K1 (Pa)	25.7e9
15	Second pressure coefficient, K2 (Pa)	-386e9
16	Third Pressure Coefficient, K3 (Pa)	12800e9
17	Third Pressure Coefficient, K3 (Pa)	12800e9

The materials had varying diameters, with the rock sample measuring 14.4 cm, the borehole measuring 6.45 mm, air measuring 5.24 mm, the polyethylene sheath measuring 4.5 mm, and PETN measuring 1.65 mm. The copper tube was securely inserted in the borehole so that gas did not enter the cracks. The explosion was triggered at the upper end of the borehole. [8] and [9] replicated the [7] experiment using the Finite Element Method, LS DYNA. The Finite Element Model (FEM) was used to replicate both the laboratory experiment conducted by [7] and the numerical simulations conducted by [8] and [9] in this paper.

The cylindrical sample was simulated using the parameters of Johnson Holmquist 2 (JH-2) constitutive law proposed by [8] and the Reidel-Heirmaier-Thoma (RHT) model proposed by [9]. To accurately resolve problems with large deformation, the ALE methodology was employed instead of the classical Lagrangian FEM. In the context of the ALE formulation, the finite element mesh experiences independent motion from the material flow. Similarly, each element within the mesh can potentially comprise a mixture of two or more different

materials. In the ALE formulation, the finite element mesh experiences independent motion from the material flow. Similarly, each element within the mesh can potentially comprise a mixture of two or more different materials.

FEM was used to model the explosion in rocks. Firstly, attempt was made to replicate the results of [7] experiment using the same materials as in the experiment. Two different constitutive models were used separately to model the rock. The first model was created with the material parameters used by [8] with JH-2 model and the second model was created with the material parameters used by [9] with RHT model. The dimensions of the rock, copper, Polyethylene, air and PETN were the same as that of the experiment. The mesh size used was 1mm x 1mm x 5 mm for all the elements. The rock and copper were modelled using Lagrangian formulation. The PETN, air, Polyethylene was modelled using the ALE. A total of 636647 nodes and 612900 elements were used in the model. Figure 3 shows the 3d view of the created FEM model. Figure 4(a) shows the plan view of the FEM model whereas Figure 4(b) shows the exploded view at the center of the model. The green color indicates the PETN (explosive), Black color indicates Polyethylene, Pink color indicates air, Purple color indicates Copper while the red color indicates rock.

The simulation of material deformation followed a two-step procedure: initially, the solid mesh underwent deformation through the application of the Lagrange method, and subsequently, the state variable of the Lagrangian element was transmitted to the entirety of the ALE mesh space. The ALE method was utilized as a means of fluid-structure interaction (FSI) to enable interaction between the moving explosive and the solid material.

The nodes at the interface between the materials were merged, forming ALE layers that constituted an ALE multi-material group (AMMG). Within the ALE parts, these materials could flow across the meshes without causing any deformation, and their movement followed advection algorithms. To simulate fluid-structure interaction (FSI), a coupling algorithm was employed using the "Constrained Lagrange in Solid" keyword in Finite Element Modeling (FEM) to replicate the contact between the materials.

PETN explosive was detonated at time $t=0$ from the bottom of the sample similar to the experiment. The model was terminated after 1×10^{-4} seconds. Hourglass control type 3 was used for the Lagrangian elements and Control type 1 was used for the ALE elements. Solid Section Element Formulation 1 was used for Lagrangian elements and Solid Section Formulation 11 for simulating the ALE elements. Free boundary conditions were used for similarity with the experiments. SI units were used for the model, i.e. meters for length, seconds for time and kg for mass.

JH-2 Constitutive Model For Rock: The Johnson Holmquist-2 (JH2) plasticity damage model is frequently utilized to replicate the characteristics of materials like ceramics, rocks, and other substances renowned for their brittleness. It was first proposed by [10]. The original JH2 model includes elements related to pressure-sensitive strength, properties associated with damage and fracture, post-fracture strength, bulking influences, and the impact of strain rate [10]. Nonetheless, the model lacks the capability to account for

gradual strain softening, a feature that may not be suitable for certain ceramic materials. The modified JH-2 model was created as an adaptation of the original JH-1 model. The constitutive model is implemented as Material 110 in FEM. The parameters of JH-2 model in this study is used as per [8] and is shown in Table 6.

RHT Constitutive Model for Rock: The RHT (Reidel-Heirmaier-Thoma) model represents an advanced damage plasticity formulation designed for brittle materials, which was first proposed by [11] for studying the dynamic loading of concrete. This constitutive model was then firstly implemented in LS-DYNA code in 2011 [12] for modeling more brittle materials like rock. The RHT model is described by the three separate surfaces, namely, the failure surface, the yield surface, and the residual surface, all contributing to the characterization of the material's strength model. In this model, when the stress reach [12] the residual surface the material is fully damaged, and the strength is determined by a residual surface. The constitutive model is implemented as Material 272 in the FEM. The parameters of JH-2 model in this study is used as per [9] and is shown in Table 5.

Explosive: Material High Explosive Burn along with the Jones Wilkins Lee, Equation of State is used in the numerical simulation. The explosive used in the blasting operation is modeled in FEM by Material type 008 together with Jones-Wilkins-Lee EOS s used to describe the explosive as it is the most popular one and the easiest to calibrate. The parameters of the PETN explosive used in this study is as per [8] and is shown in Table 1.

Air Model: In the modeling procedure, the air is described as an ideal gas, utilizing the Material NULL model and a linear polynomial Equation of State (EOS). The parameters of Air in this study is used as per [8] and is shown in Table 4.

Copper Model: The Johnson-Cook Model, which is employed in this paper for defining the copper material properties, is a metal constitutive model that relies solely on empirical data. The parameters of Copper used in this study for the Johnson Cook Model is used as per [8] and is shown in Table 3.

Polyethylene model: Polyethylene was modeled with Material Null with Equation of state, Gruneisen. The parameters of Polyethylene is used as per [8] and is shown in Table 2.

Table 7: Comparison of Jh-2 model and RHT model for the cracks in bottom

Description	JH-2 model	RHT model
Crushed zone diameter	16 mm	16 mm
Radial Cracks	8	14
Circumferential Cracks	More	Few

Table 8: Comparison of Jh-2 model and RHT model for the cracks in top

Description	JH-2 model	RHT model
Crushed zone diameter	16 mm	16 mm
Radial Cracks	negligible	8

Results of the Study: The numerical results depict the presence of cracks through the utilization of damage contours that span from 0 to 1. The color blue signifies fringe level 0, indicating the absence of damage in the rock, while the color red signifies

fringe level 1, indicating complete damage in the rock. In essence, the red contour denotes the area of crushing, while the green contour represents the circumferential and radial cracks. The remaining colors, which correspond to fringe levels 0 and 1, signify varying degrees of damage in the rocks.

Figure 5(a) and Figure 6(a) show the cracks in the top and the bottom of the sample from the [7] experiment. Figure 5(b) and Figure 6(b) show the damage pattern in the top and the bottom of the sample respectively from Wang,2018. Figure 5(c) and Figure 6(c) shows the top crack from JH-2 model whereas Figure5(d) and Figure 6(d) show the damage pattern from RHT model.

It can be seen from the above figures that the results of our 3D model match well with that obtained from the experiment and the simulation , both for the top and bottom. The patterns of cracking are very similar. Furthermore, the nature of damage is such that the Crush zones are produced in the vicinity of the blast holes, and radial cracks emanate towards the outer boundaries upon detonation. The degree of damage decreases gradually with increasing distance from the blasthole. Near the blasthole, damage takes on a crossing pattern, while in the more distant area, it assumes a radial pattern, ultimately leading to the development of a fractured region.The cracking in the bottom of the model is more than that in the top . This is very similar to the (Banadaki, 2010) experiment.

Both the JH-2 model and RHT model are successful in predicting the pattern of cracks. In the bottom of the model, crack patterns are similar. Both RHT model and JH-2 model generated similar crushed zone indicated by the red color in Figure 6(c) and Figure 6(d).However, the RHT model generated more radial cracks ,indicated by green color, compared to the JH-2 model. Further, There are more circumferential cracks in the JH-2 model compared with the RHT model. The circumferential cracks were not generated by the RHT model. The comparison between the two models is shown in Table 7.

The damage pattern in the top of the model between RHT and JH-2 model can be seen in the Figure 5(c) and Figure 5(d). The crushed zone, indicated by the red zone is very similar. However, negligible radial cracks are generated by JH-2 model compared to the RHT model, which generated more radial cracks and is in similarity to the experimental results.The comparison between the two models is shown in Table 8.

The close similarity between the experimental results and the numerical simulation proves that both the JH-2 model and RHT model can be used for simulating the explosion process of rocks, provided that the parameters are carefully calibrated. However, RHT model can be better in predicting the damage due to to close similarity in the cracking and the damage pattern with the experimental results.

3. Discussion and Conclusion

To accurately understand the explosion process in the rocks through numerical simulation, it is necessary to understand the constitutive models for rocks. There are various constitutive models available for modeling the rock. Among them, two common models are JH-2 damage model and RHT

model. Two separate numerical models were created with the JH-2 and RHT constitutive models. It helped to compare two common constitutive models for simulating the brittle behavior of rock materials, JH-2 model and RHT model. Both models performed well in simulating the cracks compared to a laboratory experiment. However, more cracks comparable to the experiment was found with the RHT model. Therefore, RHT model is better for simulating the rock blast than JH-2 model for future numerical models.

References

- [1] L X Xie, W B Lu, QB Zhang, QH Jiang, M Chen, and J Zhao. Analysis of damage mechanisms and optimization of cut blasting design under high in-situ stresses. *Tunnelling and Underground Space Technology*, 66:19–33, 2017.
- [2] Laddu Bhagya Jayasinghe, Junlong Shang, Zhiye Zhao, and ATC Goh. Numerical investigation into the blasting-induced damage characteristics of rocks considering the role of in-situ stresses and discontinuity persistence. *Computers and Geotechnics*, 116:103207, 2019.
- [3] Jian Tao, Xing-Guo Yang, Hong-Tao Li, Jia-Wen Zhou, Shun-Chao Qi, and Gong-Da Lu. Numerical investigation of blast-induced rock fragmentation. *Computers and Geotechnics*, 128:103846, 2020.
- [4] Zhiliang Wang, Haochen Wang, Jianguo Wang, and Nuo Cheng Tian. Finite element analyses of constitutive models performance in the simulation of blast-induced rock cracks. *Computers and Geotechnics*, 135:104172, 2021.
- [5] Ali Fakhimi and Mark Lanari. Dem–sph simulation of rock blasting. *Computers and Geotechnics*, 55:158–164, 2014.
- [6] Changping Yi, Jonny Sjöberg, Daniel Johansson, and Nikolaos Petropoulos. A numerical study of the impact of short delays on rock fragmentation. *International Journal of Rock Mechanics and Mining Sciences*, 100:250–254, 2017.
- [7] Mohammad Mahdi Dehghan Banadaki. *Stress-wave induced fracture in rock due to explosive action*. University of Toronto Toronto, 2010.
- [8] Jianxiu Wang, Yao Yin, and Kamran Esmaeili. Numerical simulations of rock blasting damage based on laboratory-scale experiments. *Journal of Geophysics and Engineering*, 15(6):2399–2417, 2018.
- [9] Xudong Li, Kewei Liu, Tao Qiu, Yanyan Sha, Jiakai Yang, and Ruitao Song. Numerical study on fracture control blasting using air–water coupling. *Geomechanics and Geophysics for Geo-Energy and Geo-Resources*, 9(1):29, 2023.
- [10] GR Johnson and TJ Holmquist. A computational constitutive model for brittle materials subjected to large strains, high strain rates, and high pressures. In *Shock wave and high-strain-rate phenomena in materials*, pages 1075–1082. CRC Press, 1992.
- [11] W Riedel, K Thoma, S Hiermaier, and E Schmolinske. Penetration of reinforced concrete by beta-b-500 numerical analysis using a new macroscopic concrete model for hydrocodes. In *Proceedings of the 9th International Symposium on the Effects of Munitions with Structures*, volume 315. Berlin-Strausberg Germany, 1999.
- [12] Thomas Borrvall and Werner Riedel. The rht concrete model in ls-dyna. In *Proceedings of The 8th European LS-DYNA user conference*, 2011.